ELECTRIC NOISE MEASUREMENT

The pursuit of extremely sensitive electronic measurements is a common goal among modern scientists and engineers. The limit to the signal energy that may be detected is a result of the noise energy that competes with the signal in a detection scheme. Thus, the measurement and accurate determination of the noise energy is of crucial importance when designing or assessing any signal detection system. Noise may be defined as an unwanted disturbance superimposed upon a useful signal, which tends to obscure the signal's information content. Electronic noise limits the signal detection sensitivity of a wide range of systems such as radar, ground based and satellite communication, cellular phones, and guidance and tracking systems, as well as ultrasensitive physical measurements such as radio astronomy and gravitational wave detection.

Many different types of electronic noise have been studied and characterized. Some types are fundamental in nature and can be derived from basic physical principles. Other types of noise may be classified as technical and are the result of the electronic configuration of the read-out system of the detection or measurement process. To reduce the interference from fundamental noise sources, the physical principle should be understood so that the particular detection scheme may be optimized to minimize the noise. To reduce the interference from technical noise calls for good electronic design that maintains the linearity and stability of the electronic readout across the dynamic range of operation and the required frequency band.

A common figure of merit that is used when detecting a signal is known as the signal-to-noise ratio. It is defined as the ratio of the signal power to the noise power over the frequency band of the detection system. Filtering techniques exist to maximize the signal-to-noise ratio and are known as optimum filtering. This technique relies on knowing the form of the signal and biases the detection data at the frequencies in which the signal is strongest. However, this article focuses on the common types of electronic noise and the measurement and characterization techniques. Thus, the ways of maximizing the signal-to-noise ratio via filtering techniques will not be discussed, for further information on these methods see Refs. 1–4.

To measure the noise characteristics in an electronic system accurately, we usually use a device that can be referred to as a *null instrument.* Classic devices include a bridge circuit based on a mixer, the Dicke microwave radiometer, and the Michelson optical interferometer. These devices nominally have zero output and are highly sensitive to changes in the power level or phase delay; thus, they are able to make very sensitive measurements of either the power or phase fluctuations in the system. Modern applications of these instruments to state-of-the-art physical experiments include the study of the cosmic microwave background radiation (COBE project) (5), as well as the use of advanced microwave bridge techniques and large-scale optical interferometers for the search for gravitational waves from astrophysical sources (NIOBE, LIGO, and VIRGO projects) (6,7).

Electric noise measurements may be done in the presence or absence of a carrier signal. Modern communication systems make use of carrier signals to transmit information. For example, mobile telephone systems typically operate at a frequency around 1 GHz. The voice frequencies modulate the carrier frequency as shown in Fig. 1, then the signal is transmitted through the atmosphere by the carrier at 1 GHz. At the receiving end, the signal is demodulated back to audio frequencies. The audio signal competes with the noise in the system, and as long as the signal power is much larger than the noise power, the signal can be heard at the receiver end. There is more than one way to characterize the noise in such a system. When there is a carrier signal present, it is common to measure the noise with respect to the carrier power as a ratio. This means just a relative measurement with respect to the carrier is made, which is comparatively easy to calibrate. If no carrier is present, then it is necessary to measure the absolute noise energy present. This requires a bit more effort in calibration. It is usual to equate the noise energy

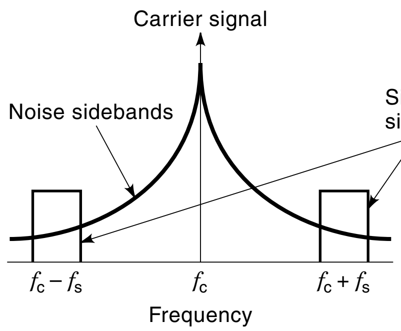

Figure 1. Spectral representation of a carrier signal with signal sidebands modulating the carrier in the presence of noise sidebands. f_C represents the carrier frequency and f_s represents the band of audio frequencies that modulate the carrier.

E_N to an effective noise temperature T_N via Boltzmann's constant, $E_N = k_B T_N$. For a system in equilibrium, this gives the fundamental relationship between the associated temperature and the energy. Basically, the more energy inside any system, the hotter it is. Likewise, when we characterize the electronic noise in a system, the higher the level of noise energy in the system, the higher the system effective noise temperature.

Many individual components make up a modern system. These include amplifiers, attenuators, mixers, and phase shifters. Each component can add to the overall system noise temperature. The common figure of merit that defines the performance of a component is the noise figure, which is equal to the ratio of the output noise density of an input source and that added by the component divided by the source alone (a full mathematical definition is given later). This type of noise characterization only characterizes the component in its small signal input regime (i.e., when no carrier signal is present). If a significant carrier signal is present, then the input power may be considered large, and the noise temperature and figure become functions of carrier power and offset frequency from the carrier. This is because many devices are nonlinear, and nonlinear up-conversions of the signal can cause a frequency dependence known as flicker noise, which can also be power-dependent. If a minimum noise temperature is essential, then we must determine the restriction to the input power that is required to maintain small signal noise performance (8).

If a communication system is designed well and is not limited by technical noise, then it usually will be limited by the noise temperature of the components in the system. The noise power in this regime is independent of the carrier power. Thus, if the carrier power can be increased without creating any noise, the signal-to-noise ratio will increase as a result of the associated increase of signal power. Recently new interferometric techniques have allowed the detection of noise in the presence of a microwave carrier to be measured at high carrier powers close to a watt, with a noise performance still governed by the system noise temperature (8,9). This technique has allowed for a factor of 10,000 improvement in sensitivity of noise energy measurements in the presence of a carrier and is expected to have a significant impact on radar and metrology design for the future.

A carrier signal is a sinusoidal tone of single frequency f_C with phase and amplitude. Thus the signal frequencies f_S may be encoded with respect to the phase or amplitude of the carrier signal, and are known as phase modulation (PM) or amplitude modulation (AM). These two "quadratures" of modulation are ideally orthogonal and, thus, are independent and may exhibit vastly different levels of noise. When noise is present in the phase quadrature, it is known as *phase noise;* when noise is present in the amplitude quadrature, it is known as *amplitude noise.* Technical noise sources usually modulate the carrier with a constant fraction of phase or amplitude independent of the carrier power. Thus, if the carrier power is increased, both the signal sidebands and the noise sidebands increase, with the signal-to-noise ratio remaining constant. This is why it is useful to characterize the phase or amplitude noise in the presence of a carrier signal by a power ratio. However, it is not the purpose of this article to dwell on AM and PM signal encoding and noise measurement techniques. More on these topics can be found in the article on MEASUREMENT OF FREQUENCY, PHASE NOISE AND AMPLITUDE NOISE. In this article, the focus is on the measurement and characterization of the small signal component noise, such as the more physically fundamental electric noise sources—thermal noise and shot noise—in the absence of a carrier signal.

Manufacturers of microwave components usually classify the noise performance in terms of the noise figure or temperature in the absence of a carrier (it is much harder to characterize the nonlinear flicker component in the presence of a carrier). Measurements of this kind are thus commonplace, and commercial noise figure test sets are available. High accuracy is available when characterizing modular components based on coaxial or waveguide input and outputs. However, the electronics industry has moved toward miniaturizing components, and many microwave circuits are produced not in modular form but rather are manufactured as part of one integrated circuit collectively called a *wafer.* Accurate characterization techniques of components "on-wafer" remains a principal concern of the metrology community and industry.

It is apparent that the accurate determination of the level of noise in a system is very important. Measurements of the noise temperature have become an art as many standards laboratories around the world strive to make their measurements of the absolute noise more accurate. The advent of the Dicke radiometer has made this possible (10). This article will focus only on the principles of noise types and measurements. To understand the principles of the radiometer the reader is referred to the article on RADIOMETERS . Recently, in the quest for more accurate measurements, an international comparison of noise temperature measurements has been undertaken between 2 GHz and 12 GHz. The institutes that took part in this comparison were: the National Institute of Standards and Technology, Boulder, Colorado, United States; the Laboratoire Central des Industries Electriques, Fontenay-aux Roses, France; the National Physical Laboratory, Teddington, United Kingdom; the Physikalisch-Technische Bundesanstalt, Braunschweig, Germany (11). The reader is also referred to the home page of these institutes for more details of state-of-the-art measurement techniques (12–15).

MATHEMATICAL REPRESENTATIONS OF NOISE

Noise is a fluctuating quantity that is described statistically by a random variable representing a fluctuating current, voltage, or power with time. When defining a random variable $X(t)$, it is important to have a measure of the extent of the fluctuations. A quantity that achieves this is known as the variance of X. To define the variance, the mean of the fluctuating quantity is first defined as $\langle X \rangle$ (it is common to use angle brackets to represent the mean of a quantity). Then a new variable representing the fluctuation about the mean can be defined, $\Delta X = X - \langle X \rangle$. Taking the mean square of this quantity defines the variance $\langle \Delta X^2 \rangle$. To calculate this quantity, we must know the probability density function $h(X)$ that describes the process. If $h(X)$ and thus the mean and variance are independent of time, the process is known as stationary.

For our purposes, the time domain representation given previously has limited use, and it is informative to introduce the Fourier method and represent $X(t)$ as a spectral density in the frequency domain. The relation between the frequency and time domains is given by the well-known Wiener–Khintchine theorem (16,17). Many undergraduate textbooks deal with this important theorem; for more details see Refs. 1, 18, and 19. The main result for our purposes is a particular case of the Wiener–Khintchine theorem that gives

$$\langle X^2 \rangle = \langle \Delta X^2 \rangle = \int_0^\infty S_x(f)\,df \tag{1}$$

for an independent stationary random process. Here, $S_x(f)$ is defined as the single-sided spectral density of the random variable, and we refer to f as the Fourier frequency. Equation (1) assumes that $\langle X \rangle = 0$, which is true for a sinusoidal variable. This term represents a direct current (dc) term and is not measured with a modern spectrum analyzer. In effect, the spectrum analyzer will set $\langle X \rangle$ to zero even if it is not.

Equation (1) gives an important result because it means that the spectral density of electronic noise may be measured very easily in principle. This can be done with a quadratic detector and a narrow band amplifier centered at the particular frequency f_0. Assuming that the bandwidth of the amplifier B_r is small in comparison to the variation in frequency of the spectral density, a constant value of $S_x(f_0)$ can be assumed. From Eq. (1), the quadratic detector will measure a voltage at the output of the amplifier equivalent to

$$\langle v^2 \rangle = G S_x(f_0) B_r \tag{2}$$

and the spectral density is easily determined. Here, G is the power gain of the amplifier, and B_r is defined as the resolution bandwidth of the spectrum analyzer.

DEFINITIONS

Flicker and White Noise

White noise is a random noise with a flat frequency spectral density over the Fourier frequency range of interest. This type of noise is usually produced in the laboratory for testing purposes. For example, white noise generators such as hot or cold resistors are used as calibrated noise sources to calibrate noise measurement systems. In general, noise in system circuits is not white and has a frequency dependence. An example of a nonwhite noise is flicker noise, which has a spectrum proportional to $1/f$ and is prevalent in many circuit systems. Generally, at large values of Fourier frequencies, system noise is white; at small values of Fourier frequencies, system noise is flicker. The frequency at which the transition occurs is known as the flicker corner, which is typically but not necessarily about 10^5 Hz.

Signal-to-Noise Ratio

In general, the signal-to-noise ratio (SNR) in a system is defined as the ratio of available signal power to available noise power present in the system over the bandwidth of detection and is given simply by

$$\mathrm{SNR} = \frac{\text{Signal power}}{\text{Noise power}} \tag{3}$$

In general, this value is dependent on the detection bandwidth. For example, if we detect a sinusoidal frequency of root mean square (rms) power S in the presence of white noise with a power spectral density of S_N (W/Hz), then the signal-to-noise ratio is given by

$$\mathrm{SNR} = \frac{S}{BS_N} \tag{4}$$

where B is the detection bandwidth. Thus, the larger the bandwidth, the larger the detected noise power, which degrades SNR. In general, the signal might consist of more than one frequency and be more complicated than a single sinusoid frequency. To optimize the SNR, a standard result in signal detection theory states that the signal-to-noise ratio is optimized by a filter that has a transfer function proportional to the complex conjugate of the signal Fourier transform divided by the total noise spectral density (1). This technique accepts frequencies where the signal is large and the noise is low and filters out frequencies where the signal is low and the noise is large. Thus, it is prudent to know the signal bandwidth when designing a detection system.

Noise Temperature

From the equi-partition theorem, a gas molecule possesses a mean energy of $k_BT/2$ J/DOF and applies also to electronics, where T is the equilibrium temperature and k_B is Boltzmann's constant. Assuming that an electronic circuit has two degrees of freedom (i.e., amplitude and phase or resistance and reactance), then the mean noise energy in a passive circuit is k_BT J. Because thermal noise is white, we may express this noise energy as a power spectral density given by $S_N(f) = k_BT$ W/Hz over all Fourier frequencies. Thus, the noise temperature at a selected frequency and reference point in the circuit may be defined as

$$T_N = S_N(f)/k_B \tag{5}$$

where $S_N(f)$ is the noise power spectral density measured or calculated at the circuit reference point and frequency. For a resistor, the noise temperature is approximately the actual temperature, whereas that observed by a diode or a transistor may be significantly larger than the absolute temperature.

Standard Reference Temperature

The standard reference temperature T_S for noise measurements is 290 K. This is an arbitrary choice; however, historically this has been chosen because it is close to room temperature.

Noise Figure

The spot noise figure (or narrow band noise figure) is defined as the ratio of the total noise power spectral density delivered to the output of the system divided by that caused by the source alone, when the source is at the standard reference temperature of 290 K. Assuming that the gain of the system is G (which may be fractional if the system has an overall attenuation), then the noise figure at a particular frequency is defined as (see Fig. 2)

$$F(f) = \frac{S_{\mathrm{N}}(f)_{\mathrm{out}}}{Gk_{\mathrm{B}}T_{\mathrm{S}}} \tag{6}$$

To calculate the overall noise figure $\overline{F}$, the spot noise figure is averaged over the frequency response of the system and is given by (18)

$$\overline{F} = \frac{\int_0^\infty F(f)G(f)\,df}{\int_0^\infty G(f)\,df} \tag{7}$$

Here $G(f)$ is now the system transfer function.

If a device is noiseless, then $S_{\mathrm{N}}(f)_{\mathrm{out}} = Gk_{\mathrm{B}}T_{\mathrm{S}}$, and both $\overline{F}$ and $F(f)$ are unity. However, for an active or dissipative device, there is some associated noise, and the noise figure is usually greater than unity. It is usual to compare noise figures in decibels ($10 \log_{10} [F]$); this is especially useful if the noise figures are close to unity.

NYQUIST'S THEOREM

When a resistor is at a finite temperature, a fluctuating current will occur as a result of random thermal motion of electrons in the resistor, which will in turn will give rise to a fluctuating electromagnetic force (emf). This is the electrical analogue to dissipative Brownian Motion giving rise to a fluctuating force. A detailed description of these principles are given in Ref. 19. This fluctuating emf was predicted by Einstein (20) and first discovered by Johnson [it is known as Johnson noise (21)]. Later, the physics was explained by Nyquist and is known as Nyquist's theorem (22).

To illustrate Nyquist's theorem, first we consider a resistance R in series with an arbitrary reactance $X(f)$, as shown

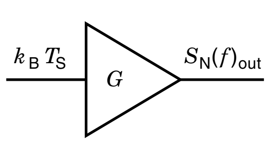

Figure 2. Schematic of a two-port device under test with the associated input and output.

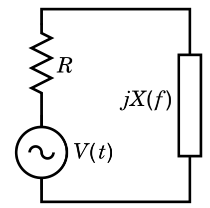

Figure 3. Model of a resistor connected in series with a reactance at temperature T. The voltage generator represents the internal Johnson noise supplied by the passive circuit.

in Fig. 3. It is known that $V(t)$ is a white noise source, and thus its spectral density $S_v(f)$ will be constant. From the Wiener–Khitchine theorem and linear circuit theory, the relation between the voltage and current spectral densities is given by

$$S_i(f) = \frac{S_v}{R^2 + X(f)^2} \tag{8}$$

Assuming $X(f)$ is inductive (we can also assume that it is capacitive and achieve the same result) and equal to $2\pi fL$, where L is the inductance, it can be shown from Eqs. (8) and (1) that

$$\langle i^2 \rangle = \int_0^\infty S_i(f)\,df = S_v \int_0^\infty \frac{df}{R^2 + 4\pi^2 f^2 L^2} = \frac{S_v}{4RL} \tag{9}$$

Now the equipartition theorem is invoked. It states the mean energy stored in an inductor (a similar equation governing the energy stored in a capacitor exists) is given by (19)

$$\frac{1}{2} L \langle i^2 \rangle = \frac{1}{2} k_{\mathrm{B}} T \tag{10}$$

By combining Eqs. (10) and (9), Nyquist's theorem is derived:

$$S_v = 4k_{\mathrm{B}}TR \tag{11}$$

This derivation gives only the classical solution and is not general for low temperatures and high frequencies. When $\hbar\omega \geq k_{\mathrm{B}}T$, there is a quantum correction and takes the form (18,19,22)

$$S_v = \frac{4\hbar\omega R}{e^{\hbar\omega/k_{\mathrm{B}}T} - 1} \tag{12}$$

where $\hbar$ is Planck's constant. When T is large Eq. (12) collapses back to the form given by Eq. (11).

EQUIVALENT CURRENT AND VOLTAGE NOISE GENERATORS

The noise at the output of a two-terminal (or one-port) network can be represented as either a noise current generator in parallel with its admittance or a noise emf in series with its impedance. The equivalent networks are shown in Fig. 4. From Nyquist's theorem, the thermal noise of a resistance R at temperature T, measured in a frequency bandwidth Δf, can be represented by the voltage generator $\sqrt{4k_B TR\,\Delta f}$ in series with a resistance R, as shown in Fig. 4(b). Likewise, the noise may be equally represented by the current generator $\sqrt{4k_B Tg\,\Delta f}$ in parallel to the resistance $R = 1/g$, where g is the conductance. Thus, the *equivalent noise resistance* or *equivalent noise conductance* of a device at temperature T_0 may be written as

$$R_n = \frac{\langle v^2\rangle}{\Delta f}\frac{1}{4k_B T_0} = \frac{S_v(f)}{4k_B T_0},\ g_n = \frac{\langle i^2\rangle}{\Delta f}\frac{1}{4k_B T_0} = \frac{S_i(f)}{4k_B T_0} \quad (13)$$

Thus, from a measure of the open circuit voltage $S_v(f)$ [V^2/Hz] or short circuit current spectral density $S_i(f)$ [A^2/Hz], the equivalent noise resistance and conductance may be calculated. Figure 4 implies that the noise spectral densities are related by $S_v(f)/S_i(f) = |Z|^2$; thus the noise conductance and resistance are in general related by

$$R_n = g_n|Z|^2 \quad (14)$$

The noise resistance and conductance can be related to the noise temperature by equating the spectral densities as follows:

$$S_i(f) = 4k_B T_n g, S_v(f) = 4k_B T_n R \quad (15)$$

Thus by equating Eqs. (15) and (13), the relation between the noise temperature, noise resistance, and noise conductance may be written as

$$T_n = \frac{g_n}{g}T_0 = \frac{R_n}{R}T_0 \quad (16)$$

The noise of the device has been expressed in terms of the temperature T_0, which is not necessarily the device temperature. This is because the device temperature is not necessarily well defined because a temperature gradient might exist, especially for active devices. Thus, it is common to define the noise characteristics with respect to the standard temperature $T_0 = T_S$ (290 K). However, if a device is passive and gives the expected thermal noise, then $T_n = T_0$, $g_n = g$, and $R_n = R$, and the device can be defined with respect to its own temperature as a reference.

It is necessary to mention here that these generators are one-port or two-terminal devices that, for example, may represent a diode or resistive noise source. If a device has more ports or terminals associated with its structure, then more than one noise generator must be considered when calculating the noise parameters. One such example is a transistor that is a three-terminal device. For example, a bipolar transistor has an emitter, base, and collector. In general, three noise generators between each terminal must be considered along with any correlated components. This article does not discuss this problem, and the reader is referred to Ref. 18 for more details. For our considerations, the noise added by a two-port system will be described by the noise figure and noise temperature concept and is discussed in more detail later.

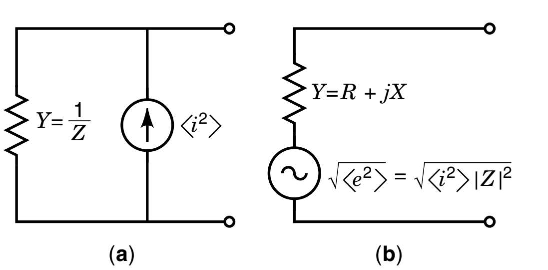

Figure 4. (a) Two-terminal network represented by a noise current generator in parallel with an admittance. (b) Two-terminal network represented by a noise voltage generator in series with an impedance.

TYPES OF NOISE

Thermal Noise

The basics of thermal noise was given previously by the Nyquist description and holds for a passive resistor as long as its temperature is in equilibrium. This description allows for the general quantification of any measurable noise power in terms of equivalent noise temperature, equivalent noise figure, equivalent noise conductance, and equivalent noise resistance. Thermal noise in a resistor is caused by the random motion of the current carriers, which produce a fluctuating voltage across its terminals. The problem can also be treated as a diffusion problem or velocity fluctuation problem of the current carriers (18). These descriptions are particularly useful when analyzing the thermal noise in a semiconductor. A semiconductor device has a nonlinear voltage current characteristic, and Nyquist's theorem holds for a p–n junction at zero bias where the resistance is considered as dV/dI at the temperature of equilibrium.

Generation and Recombination Noise

Generation and recombination noise (g–r noise) occurs in semiconductors that involve donors, traps, and recombination centers of the charge carriers. In general, the resistance of the material is dependent on the number of charge carriers; thus if the number of carriers fluctuates, the resistance will fluctuate also, causing a fluctuating voltage across the terminals. The appearance and disappearance of carriers by this process is described by

$$\frac{d}{dt}(\Delta n) = -\frac{\Delta n}{\tau} + H(t) \quad (17)$$

Here $H(t)$ is a random noise term, Δn is the fluctuation in number of carriers, and τ is the carrier life time. If we take the Fourier transform of Eq. (17) and apply the Wiener–Khintchine theorem, then the frequency domain representation can be written as

$$S_n(f) = \frac{S_H(f)\tau^2}{1+4\pi^2\tau^2 f^2} \quad (18)$$

Assuming that the spectral density of $H(t)$, S_H, is white, the value of $\langle \Delta n^2\rangle$ may be calculated from Wiener–Khintchine theorem as

$$\langle \Delta n^2 \rangle = \int_0^\infty S_n(f)\,df = S_H \tau \int_0^\infty \frac{\tau\,df}{1+4\pi^2\tau^2 f^2} = \frac{S_H \tau}{4} \quad (19)$$

Thus, by combining Eqs. (18) and (19), the spectral density of the number of fluctuating carriers can be shown to be

$$S_n(f) = \frac{4\langle \Delta n^2 \rangle \tau}{1+4\pi^2\tau^2 f^2} \quad (20)$$

The spectrum $S_n(f)$ can be calculated as soon as τ and $\langle \Delta n^2 \rangle$ are known.

Shot Noise

Shot noise occurs when there is current flow across a potential barrier. The current fluctuates around an average value as a result of a random emission of current carries across the potential barrier. This effect occurs in p–n junctions in diodes and transistors, at the cathode surface of a vacuum tube, and so on. Shot noise can be driven by thermal fluctuations or other mechanisms such as noise due to recombination centers in the space charge region. To describe shot noise, we will consider a n^+–p junction as shown in Fig. 5.

The characteristic of the current crossing the depletion (or space charge) region can be written as

$$I(V) = I_0(V)\left(\exp\left[\frac{qV}{kT}\right] - 1\right) \quad (21)$$

where q is the charge of the electron. Here, the first term in Eq. (21) is caused by electrons injected from the n^+-region to the p-region, and the second term is the reverse current caused by electrons injected from the p-region into the n^+-region. To proceed further, Schottky's theorem is invoked (23). It states that the spectral density of current fluctuations in an emission process is related to the current by

$$S_i = 2qI \quad (22)$$

for frequencies less than the inverse of the transit time. Because noise spectral densities are additive and do not depend on the direction of current flow, the spectral density of shot noise current in a p–n junction is given by

$$S_i(f) = 2qI_0(V)\left[\exp\left(\frac{qV}{kT}\right) + 1\right] = 2q[I(V) + 2I_0(V)] \quad (23)$$

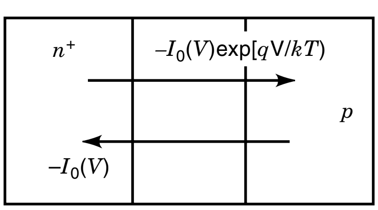

Figure 5. Current flow across the space charge region (or depletion region) in a n^+–p junction when a voltage is applied from the p^* to n^+ terminal. The separation of charge in the space charge region causes an internal electric field that has the potential to create shot noise. The arrows show the direction of the electron flow, which is in the opposite direction of the current flow.

Applying some algebra, it is also common to write Eq. (23) as

$$S_i(f) = 2qI \frac{\left[\exp\left(\frac{qV}{kT}\right) + 1\right]}{\left[\exp\left(\frac{qV}{kT}\right) - 1\right]} = 2qI \coth\left(\frac{qV}{kT}\right) \quad (24)$$

or

$$S_i(f) = 2kTg_0\left(\frac{I+2I_0}{I+I_0}\right), \text{ where}, g_0 = \frac{dI}{dV} = \frac{q(I+I_0)}{kT} \quad (25)$$

At zero bias, the conductance g_0 supplies the equivalent of full thermal noise as Eq. (25) reduces to $S_i(f) = 4kTg_0$, and half this value when $I \gg I_0$. A similar equation can be written for the open circuit voltage noise spectrum. At high frequencies, the transit time across the depletion region must be considered. This is cumbersome and will not be discussed here; the reader is referred to some standard texts (18,24) to understand this effect. Also, at low temperatures and high frequencies quantum shot noise must be considered just as quantum Nyquist noise was considered previously. Consideration of this effect can be found in Ref. 25.

It should be pointed out here that not all currents exhibit shot noise. If the arrival time of charge carriers are correlated and not random, then suppression occurs. Common examples are space charge limited emissions from a tube and a chemical battery (26). Also, if we design a feedback control system to detect and cancel the noise below, shot noise may be attained. This type of system will then be limited by the noise in the detection system.

Flicker Noise

At large Fourier frequencies most devices can be explained in terms of thermal or shot noise processes. However at small Fourier frequencies excess noise exists. Usually, low-frequency noise has an $f^{-\alpha}$ dependence where $\alpha \sim 1$, and is known as *flicker noise*. The frequency at which the flicker noise is equal to the normal white noise is known as the flicker corner f_C and can vary considerably from device to device. Also, it is not always constant because it can depend on the operating conditions such as input power and bias voltage. Also, it does not in general decrease with temperature as thermal and shot noise do. Similar components made from the same manufacturer can have very different levels of flicker noise, which suggests that it is associated with the fine details and is not under the manufacturer's control.

Flicker noise can be enhanced in nonlinear and chaotic systems, thus it is always prudent to try to maintain the linear operation of a device to keep the flicker noise to a minimum. Recently, a interferometric method, which significantly reduces the effects of flicker noise, was developed at microwave frequencies and is discussed later.

Flicker noise in general cannot be precisely calculated; instead it is common to introduce the noise model in terms of the white power spectrum S_w

$$S_f(f) = S_w\left(1 + \frac{f_c}{f}\right) \quad (26)$$

In general, no single model can describe the physical principles of flicker noise, unlike shot and thermal noise. However,

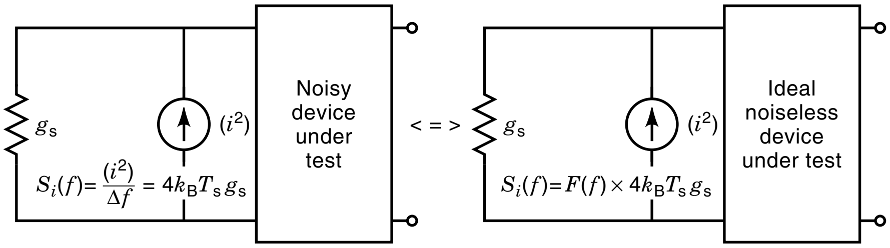

Figure 6. A standard noise source ($4k_BT_sg_s$) at the input of a noisy device under test may be represented as an enhanced noise generator at the input of an ideal noiseless device under test. The enhancement factor $F(f)$ is in general frequency dependent and known as the "spot noise figure."

specific descriptions of flicker noise have been made based on surface and generation and recombination effects (27), quantum effects (28–30), and number and mobility fluctuations (31–33). No attempt will be made to explain these specifics, and the reader is referred to the cited references.

A model worth mentioning is a result of a continuous distribution of time constants (34). A process with a single relaxation time τ_j will have a power spectral density of

$$S_j(f) = \frac{4A_j\tau_j}{1+(2\pi f\tau_j)^2} \tag{27}$$

At low frequencies, Eq. (27) varies as $1/f^2$ so flicker noise cannot be explained in terms of a single relaxation time process. However, assuming a distribution of relaxation times in the frequency range $1/\tau_2 \ll 2\pi f \ll 1/\tau_1$, the power spectral density can be shown to be

$$S_j(f) = \left[\frac{A}{2\pi \ln\left(\frac{\tau_2}{\tau_1}\right)}\right]\left[\frac{\tan^{-1}(2\pi f\tau_2) - \tan^{-1}(2\pi f\tau_1)}{f}\right] \tag{28}$$

This spectrum is constant at very low frequencies—$1/f$ for an intermediate range and $1/f^2$ for high frequencies. The model given by Eq. (26) cannot be true for very low frequencies because if the spectrum is integrated between 0 and ∞, it diverges at both limits. Therefore, there must be a lower frequency, in which Eq. (26) is no longer valid and the spectrum varies slower than $1/f$, and an upper frequency, in which Eq. (26) varies faster than $1/f$; Eq. (28) fits this requirement. However, flicker noise in some systems can still be measured in the submicrohertz regime, and thus many processes must have long relaxation times indeed. However, we know that this should at least be limited by the age of the universe!

Burst Noise

Burst noise (also known as popcorn noise) occurs in semiconductor devices and is the result of a defect in manufacturing. The waveform typically consists of random pulses of variable length and constant height (35) and can be described by a random switch model (36). The mechanism of the burst is the result of edge dislocations in the emitter space charge region (37) resulting from lattice distortions caused by large emitter doping densities and metallic impurity. The way to reduce this effect is to keep doping densities below the critical density and to improve manufacturing process. The spectral density of the noise is typically $1/f^{\gamma}$, where γ is typically 2.

NOISE FIGURE AND TEMPERATURE OF A DEVICE UNDER TEST

To measure the noise in a system, a standard noise source is introduced at the input, as shown in Fig. 6. Referring the device noise to the input of the device under test means that the equivalent enhanced current generator gives a noise output power of $F(f)$ times more than the reference temperature generator. This quantity is the spot noise figure defined in Eq. (6).

The spectral density of the equivalent enhanced current generator may be written as

$$S_i(f) = F(f)4k_BT_sg_s = 4k_BT_sg_s + [F(f)-1]4k_BT_sg_s \tag{29}$$

The first term of the left-hand side in Eq. (29) is the thermal noise of the reference source and the second term is the noise of the device under test. The device is noiseless if the noise figure is unity; in this case, the only noise present in the system is the noise of the source. If the device under test adds the same level of noise as the reference, the noise figure is two.

To relate the noise figure to the noise temperature, $T_{\mathrm{n\,DUT}}$, of the stage represented by the device under test, the second term on the left-hand side in Eq. (29) may be written as

$$[F(f)-1]4k_BT_sg_s = 4k_BT_{\mathrm{n\,DUT}}g_s \tag{30}$$

This means that the noise figure and temperature are related by

$$T_{\mathrm{n\,DUT}} = [F(f)-1]T_s \tag{31}$$

The advantage of the noise temperature notation is that if noise sources are uncorrelated, then noise temperatures are additive. The equivalent noise temperature of the system of Fig. 6 is thus given by $T_{\mathrm{eq}} = T_s + T_{n\,\mathrm{DUT}}$, and the spectral density of the equivalent current generator from Eq. (29) may also be represented by

$$S_i(f) = 4k_BT_{\mathrm{eq}}g_s \tag{32}$$

When dealing with microwaves, it is more common to consider the noise as a power spectral density rather than a voltage or current spectral density. Microwave circuits are usually matched with the standard impedance of 50 Ω. The available power at the output of the noise source is defined as the power fed into a matched load, and the equivalent circuit of a source connected to a load is shown in Fig. 7. If $g_l = g_s$,

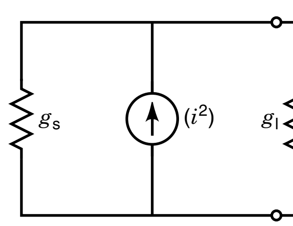

Figure 7. Equivalent current generator of a resistor of conductance g_s with a resistive load g_l at the output.

then the current will be split into both resistances equally and the available noise power at the load will be

$$N_{\mathrm{av}} = \frac{\langle i^2 \rangle}{4g_{\mathrm{s}}} \tag{33}$$

Given that $S_i(f) = \langle i^2 \rangle / \Delta f = 4k_{\mathrm{B}}T_{\mathrm{s}}g_{\mathrm{s}}$, then the power spectral density of the available noise power will be

$$S_N = N_{\mathrm{av}}/\Delta f = k_{\mathrm{B}}T_{\mathrm{s}} \tag{34}$$

This formula is similar to the initial definition of noise temperature in Eq. (5) (i.e., if we measure the noise power spectral density referred to the input of a device, then to calculate the noise temperature, we simply divide the spectral density by Boltzmann's constant).

In reality, devices are never perfectly matched; the effect of a mismatch in the context of a scattering matrix and reflection coefficient description will be discussed later. Also, the noise temperature and generator concept can be generalized to multiport devices, and in general correlations between noise sources must be considered. This will not be presented in this article, and the reader is referred to the literature (38).

NOISE FIGURE AND TEMPERATURE OF CASCADED STAGES

If two networks of noise temperature T_{N1} and T_{N2} and power gains G_1 and G_2 are cascaded and fed by a noise source of temperature T_{s} at the input of the first, then the output noise density is given by

$$\begin{aligned} S_{\mathrm{N}}(f)_{\mathrm{out}} = G_1(f)G_2(f)k_{\mathrm{B}}T_{\mathrm{s}} + G_1(f)G_2(f)k_{\mathrm{B}}T_{\mathrm{N1}} \\ + G_2(f)k_{\mathrm{B}}T_{\mathrm{N2}} \end{aligned} \tag{35}$$

To refer the noise to the input of the first stage, the noise power must be divided by the total gain $G_1(f)G_2(f)$, and the equivalent noise power density at the input is

$$S_{\mathrm{N}}(f)_{\mathrm{in}} = k_{\mathrm{B}}\left(T_{\mathrm{s}} + T_{\mathrm{N1}} + \frac{T_{\mathrm{N2}}}{G_1(f)}\right) \tag{36}$$

Thus, the equivalent noise temperature of the system is given by

$$T_{\mathrm{eq}} = T_{\mathrm{s}} + T_{\mathrm{N1}} + \frac{T_{\mathrm{N2}}}{G_1(f)} \tag{37}$$

For the single stage introduced in the last section, it was noted that the noise temperature is additive. In general for cascaded networks, the noise temperature must be normalized by the preceding gain before it is summed. In general for a cascade of m networks,

$$T_{\mathrm{eq}} = T_{\mathrm{s}} + T_{\mathrm{N1}} + \sum_{j=2}^{m}\left(\frac{T_{\mathrm{N}j}}{\prod_{i=1}^{j-1} G_i(f)}\right) \tag{38}$$

The noise figure for the cascaded network when $m = 2$ is given by

$$F_{\mathrm{eq}}(f) = \frac{S_{\mathrm{N}}(f)_{\mathrm{in}}}{k_{\mathrm{B}}T_{\mathrm{s}}} = 1 + \frac{T_{\mathrm{N1}}}{T_{\mathrm{s}}} + \frac{T_{\mathrm{N2}}}{G_1(f)T_{\mathrm{s}}} \tag{39}$$

where $T_{\mathrm{s}} = 290$ K. Combining the relationship between noise figure and noise temperature for a single network derived previously in Eq. (31), the following is obtained:

$$F_{\mathrm{eq}}(f) = F_1(f) + \frac{F_2 - 1}{G_1(f)} \tag{40}$$

This may be generalized to a system consisting of m cascaded networks and is given by

$$F_{\mathrm{eq}}(f) = F_1(f) + \sum_{j=2}^{m}\left(\frac{F(f)_j - 1}{\prod_{i=1}^{j-1} G_i(f)}\right) \tag{41}$$

This equation is known as Friis's formula (39).

NOISE FIGURE AND TEMPERATURE OF LOSSY TRANSMISSION LINE

When a system has a significant length of transmission line, which may be at different temperatures, then the losses may significantly contribute to the equivalent noise temperature of the system. Examples of this type can occur when undertaking cryogenic measurements of a device under test. If the noise source is at room temperature, then the transmission line must connect to the input via a long cable with a temperature gradient. Another example is a link connecting a satellite ground station antenna and a low noise amplifier. In this section, the physical temperature will be denoted by T and the noise temperature by T_{N}.

First, a piece of transmission line at temperature T and loss L, where $L = 1/G$, is considered. There are two ways in which the transmission line can degrade the noise performance of a system: (1) The loss attenuates the signal and thus effectively enhances the noise temperature of the following stages [see Eq. (38)]; (2) The lossy system is itself a noise generator in a similar way to a resistor (i.e., it generates Nyquist noise). This noise is dependent only on the dissipated power.

The noise generated by the transmission line is dependent on the power lost in transmission (i.e., the power dissipated). The fraction of power that is transmitted is equal to $1/L$ (or G) and thus by conservation of energy, the fraction of dissipated power must be equal to $(1 - 1/L)$ or $(1 - G)$. Thus the available noise power density at the output of a lossy transmission line with a standard noise source of T_{s} at its input will be

$$S_{\mathrm{N}}(f)_{\mathrm{out}} = G_1k_{\mathrm{B}}T_{\mathrm{s}} + (1 - G_1)k_{\mathrm{B}}T_1 \tag{42}$$

The second term in Eq. (42) is the contribution of the first piece of transmission line after the source input (denoted by subscript 1). To calculate the effective noise temperature refer to the input of the transmission line, T_{N1}; this term must be equated with $G_1k_{\mathrm{B}}T_{\mathrm{N1}}$ and can be calculated to be

$$T_{\mathrm{N1}} = \frac{(1 - G_1)}{G_1}T_1 = L_1\left(1 - \frac{1}{L_1}\right)T_1 \tag{43}$$

From Eqs. (43) and (31), the noise figure of the transmission line may be calculated to be

$$F_1(f) = 1 + (L_1 - 1)\frac{T_1}{T_s} \tag{44}$$

If a transmission line is without loss, it will not add any extra noise to the system. However, if it is not, then the second term in Eq. (44) represents the extra noise resulting from the power dissipation. Also, if there are any other networks cascaded after the lossy line, the noise added when referred to the input of the transmission line will be degraded by its loss L (or $1/G$).

If a lossy transmission line exists in a system under measurement, it may be considered as a separate network among a cascaded system and treated as in the previous section. This gives a method for correcting for any significant transmission line losses if they are known.

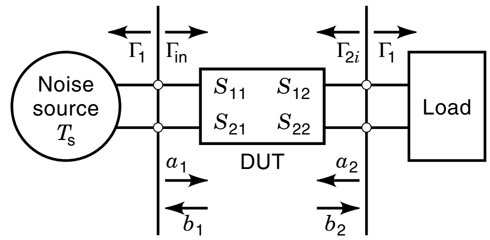

Figure 8. Schematic of the noise temperature measurement of a device under test such as an amplifier. In general, the model uses either the reflection coefficient Γ concept or the scattering parameter S_{ij} concept. Many modern undergraduate textbooks discuss these concepts so they are not explained here.

TWO-NOISE SOURCE METHOD

The two-noise source technique makes use of connecting two different known noise sources to the input of a device under test and measuring the change in output (40). It is assumed that two known noise sources of temperatures T_h and T_c are connected in turn to the input of the device under test. In this case, the ratio of output power from the two sources will be equal to

$$Y = \frac{T_e + T_h}{T_e + T_c} \tag{45}$$

where T_e is the effective noise temperature of the device under test. (This is the same as T_N introduced previously, however, to be consistent with the literature for this technique we will use T_e.) Thus

$$T_e = \frac{T_h - YT_c}{Y - 1} \tag{46}$$

This is referred to as the operational definition of T_e (40).

This method assumes perfect matching between components. In reality, the measurement technique is made more complicated if mismatches occur between the source and device under test. To characterize the mismatch requires the use of more sources and a more complicated measurement procedure and is discussed in the next section.

EFFECTS OF MISMATCH

When considering the effect of mismatch on noise measurements of a device under test, it has been useful to use a scattering matrix or reflection coefficient method to describe the measurement (41,42). Mismatch effects are pronounced when measuring amplifiers because the optimum input impedance is not the same as the matching condition for maximum power flow. For this reason, it is common for a low-noise commercial amplifier to come with an isolator at the input. Complications in the measurement procedure occur because not only does the mismatch change the level of available power, but it also means that reflections will occur at two planes, as shown in Fig. 8. Consequently, reverse flow of power through the device under test must be considered. In the previous analysis, it was always assumed that the flow of power was one way (i.e., from the source to the output of the device under test). In general, the value of noise temperature is dependent on the mismatch, and to characterize the system completely, four independent parameters must be measured (43–46). There are two common approaches with different parameter sets that warrant further discussion.

Noise Parameter Set $T_{e(min)}$, R_n, and Γ_{opt} (Complex)

The dependence on the reflection coefficient at the input port between the source and the device under test must be corrected for, and it has been traditional to use the four standard IEEE parameters given to characterize this correction. To solve for the four parameters, at least four different noise sources are needed, but it is advantageous to have more to allow averaging and to help ensure a unique solution. The classical way of measuring these parameters relies on using tuners on each end of the device under test to simulate the input and output matching networks when calibrating the system (47–50). This method relies on scalar information only and is sometimes unreliable. To determine the noise parameters more accurately, a vector network analyzer is needed to calculate the device under test scattering parameters and the reflection coefficient of the receiver (50).

T_e may be written in terms of $T_{e(min)}$, R_n, and Γ_{opt} (contains two parameters because it is complex) as

$$T_e = T_{e(min)} + \frac{4T_s R_n G_{opt}|\Gamma_1 - \Gamma_{opt}|^2}{(1 - |\Gamma_{opt}|^2)(1 - |\Gamma_1|^2)} \qquad \text{where} \quad G_{opt} = \frac{(1 - |\Gamma_{opt}|^2)}{Z_0|1 + \Gamma_{opt}|^2} \tag{47}$$

Here, T_s is a reference temperature (typically 290 K), Z_0 is the characteristic line impedance (normally 50 Ω for a microwave coaxial system). $T_{e(min)}$ is the minimum effective input noise temperature, which is realized when $\Gamma_1 = \Gamma_{opt}$, and R_n characterizes how quickly T_e increases above $T_{e(min)}$.

Noise Parameter Set T_a, T_{rev}, and β (Complex)

This set of parameters, developed at NIST (43), is useful because they are terminal invariant (i.e., their values do not change if a lossless two port is added or subtracted from the input). The method was developed to enable a direct measurement of one of the parameters, namely T_{rev}, the noise temperature of the radiation emerging from the input. Recently this method was shown to give an accuracy of ± 0.04 dB when measuring commercial low-noise microwave amplifiers (51). However, a disadvantage is that it requires skill in low-temperature measurements because T_{rev} is typically at cryogenic temperatures for a low-noise amplifier.

T_{e} can be expressed in relation to this model as

$$T_{\mathrm{e}} = \frac{T_{\mathrm{a}} + T_{\mathrm{rev}}|\Gamma_i' - \beta|^2}{1 - |\Gamma_i'|^2} \tag{48}$$

where

$$\Gamma_i' = \frac{\Gamma_1 - S_{11}^*}{1 - S_{11}\Gamma_1}$$

Here, S_{11} is the input scattering parameter to the device under test (see Fig. 8), T_{rev} is the available noise power from the internal noise sources when the output of the amplifier is terminated in a noiseless matched load, β is a measure of the correlation of the available noise power emanating from the two amplifier ports, and T_{a} is the amplifier noise temperature if no mismatch exists at the amplifiers input.

As before, this method still requires accurate determination of scattering parameters and reflection coefficients using a vector network analyzer, as well as at least four different sources to determine the four parameters. However, it is also common to use more than four noise sources to add some redundancy to improve the accuracy of the experiments (46,51,52).

For a properly made measurement when mismatch is corrected, the major source of inaccuracy is the accuracy to which the noise source is calibrated. Other noise parameters are obtained from relative measurements and are not affected by noise source calibration errors. This fact has led some of the world's national metrological institutes to do a comparison of noise source calibration and is discussed later.

NOISE SOURCES

Calibrated noise sources are essential if accurate noise measurements as discussed previously are to be made. Noise sources may be categorized as either primary or nonprimary.

Primary Noise Standards

Primary noise standards are thermal noise sources that include a resistive device held at a known temperature. Examples include cooled coaxial resistive terminations immersed in liquid nitrogen at its boiling temperature (cold standard), high-temperature oven standards that operate at typically 500 K to 800 K (hot standards), and room temperature standards that operate at about 290 K. More information on these types of standards can be found in Refs. 53–59. The measurement and characterization relies on knowing the calculable output noise power of a black body radiator such as SiC at cryogenic temperatures or the known temperature and resistance of a passive termination.

Other noise sources can be classified as nonprimary and are usually calibrated against a primary standard if accurate measurements are to be made. They include gas discharge tubes, solid-state diode sources, and commercial "cold load" thermal noise sources operating at liquid nitrogen temperature as well as "hot load" noise sources operating at elevated temperatures. Because we have already discussed in detail thermal noise, only the former two will be discussed further.

Diode Noise Sources

In forward bias, a diode produces shot noise and may be used as a noise source. However, at high frequencies such as microwave, the noise is reduced as a result of transit time effects. Also, flicker noise is present. This means that a white noise spectrum is not generated so the effective noise temperature is a function of Fourier frequency.

Another way a diode may be used to produce noise is to reverse bias the diode near the breakdown (or avalanche) region. Such noise sources give white noise up to the gigahertz region and can be used as wide-band noise sources. They are relatively small devices that require only small voltages and operate with noise temperatures of order 10^4 K. The diode itself has a $T_{\mathrm{N}} = 10^5$ to 10^6 K, which is reduced by a sizeable attenuator used to provide matching. These types of noise sources need calibration, remain calibrated for long times, and are available commercially.

Gas-Discharge Noise Sources

Gas discharges become electrical conductors at high temperatures. Typically a gas discharge tube consists of an ionized noble gas at low pressure. High voltages across the tube are necessary to create the discharge. Typically, these devices produce a discharge with excellent long-term stability that is practically independent of operating conditions, which varies little from tube to tube. The available noise power exhibits a flat power spectrum and an effective noise temperature of order 10^4 K. To make use of the noise generation at microwave frequencies, the tube can be mounted in a microwave waveguide.

INTERNATIONAL COMPARISON OF THERMAL NOISE TEMPERATURE MEASUREMENTS

The world's major state-of-the-art metrological institutes are the places where the most accurate measurements of absolute noise temperature can be made. Recently, an international comparison was undertaken to measure the noise temperature of two commercial microwave noise sources to try to obtain a measure of the absolute error (11). The institutes that took part were the National Institute of Standards and Technology in Boulder, Colorado, United States (13); the Laboratoire Central des Industries Electriques in Fontenay-aux Roses, France (14); the National Physical Laboratory in Teddington, Worcestershire, United Kingdom (12); and the Physikalisch-Technische Bundesanstalt in Braunschweig, Germany (15).

The measurements required each institute to provide its own noise standard and radiometer to preform measurements at three different frequencies. Two entirely different primary standards (cryogenic and oven) were implemented, along with two different types of radiometer (switching and total power). Uncertainties (2σ) between the institutes ranged from 0.5% to 2.9%. Expense and effort was required to fix the primary standards and sources under measurement at a fixed operating temperature. This achievement represents the best determination of absolute measurement uncertainties.

ON-WAFER NOISE MEASUREMENTS

The advent of intgrated circuits designs on a single chip has enabled the industry to miniaturize circuits and reduce the expense of microwave and millimeter wave technologies. Collectively, a circuit of this type is often referred to as a *wafer*. The characterization of such devices is more challenging than the waveguide or coaxial counterpart because it is harder to isolate a single device in a wafer. Moreover, impedance matching the device under test to the measurement apparatus is difficult, and these characterizations are always implemented in a large mismatch environment. For accurate measurement, it is important to have a vector network analyzer, which is calibrated for S-parameter measurements. The measurement process is quite intensive because it requires the measurement of the S-parameters of the noise source, noise receiver, adaptors, probes, and the like.

Much work has been done to develop on-wafer techniques (50,60–63). Commercial systems exist; however, work still is being pursued to assess the accuracy and reliability of such measurements, and ways of improving on-wafer measurements are still under investigation. The chief problem arises as a result of the mismatch and loss of the adaptor to coaxial and waveguide noise standards. To reduce these errors, on-wafer calibrated noise standards are needed. Measurements have been achieved with off-wafer noise standards, and some initial steps using on-wafer uncalibrated noise sources have been achieved (64,65). Other problems include radiation entering the open stripline format of a wafer.

INTERFEROMETRIC NOISE MEASUREMENTS

Previous discussions have mainly been about noise temperature and figure measurements of a device under test (DUT) when it is operating in the small signal regime (i.e., with no carrier signal present). A large carrier signal can cause nonlinear effects such as up-conversions, which enhance noise at small values of Fourier frequency (offset from the carrier). Recently, interferometric measurement and signal generation schemes at microwave frequency have been developed (8,9) and allow component characterization and operation at the intrinsic small signal noise temperature independent of the carrier power. The basic noise measurement setup is shown in Fig. 9. It includes the microwave interferometer consisting of the DUT and a compensating branch that enables the cancellation of the carrier at the dark fringe of the interferometer. The signal without the carrier is then amplified by the low-noise microwave amplifier operating in the small signal regime. The low-noise microwave amplifier and a mixer form the microwave readout system, which can be either phase- or amplitude-sensitive depending on the setting of the reference phase shifter φ_{ref}.

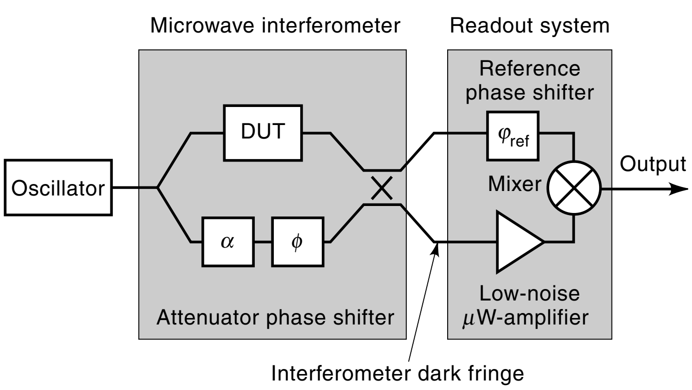

Figure 9. Schematic of the microwave interferometer measurement system of a DUT in the presence of a carrier frequency.

One of the features of the interferometric measurement system is a greatly enhanced sensitivity to phase and amplitude fluctuations of the DUT. The sensitivity enhancement results from the ability of interferometric system to satisfy, on the first glance, two contradictory requirements: (1) having a high power at the input of the interferometer, and (2) enabling low-noise operation of the readout system. These requirements are met by interfering the two signals destructively from the output of the DUT and compensating branch (suppressing the carrier) before the noise is detected by the readout system. This enables the microwave amplifier in the readout system to operate in the small signal regime devoid of flicker noise and reduces the effect of the mixer flicker noise by the amplifier gain.

The effective noise temperature of the readout system T_{RS} limits the sensitivity of the interferometric noise measurement system, and the noise temperature is given by

$$T_{\text{RS}} = T_0 + T_{\text{a}} + \frac{T_{\text{m}}}{G_{\text{a}}} \tag{49}$$

where $T_0 \approx 290$ K is the ambient temperature; T_{a} and T_{m} are the effective noise temperature of the microwave amplifier and mixer, respectively; and G_{a} is the gain of the microwave amplifier. In general, T_{RS} is a function of Fourier frequency f and the power at the input of the low-noise microwave amplifier. This dependence is caused by the amplifier flicker noise, which generally scales proportionally with input power (66,67). Suppressing the carrier at the interferometer output minimizes the degradation of T_{RS} as a result of the amplifier flicker noise, and choosing an amplifier with a low level of Johnson noise allows the measurement to be close to ambient temperature. There is some conflicting data published (68) that suggests flicker noise in amplifiers can be reduced as input power is increased. However, when the input to the amplifier is totally nulled, the resulting noise spectrum is white and devoid of flicker noise, and this represents the optimum operating condition.

These types of measurements are relatively new; consequently, the accuracy has not been determined, and mismatch correction techniques have not yet been applied.

ACKNOWLEDGMENTS

The author thanks Dr. Eugene Ivanov and Richard Woode for reading the manuscript and helping with references. He also thanks the Librarian Will Hamilton for his patient help in finding reference material.

BIBLIOGRAPHY

1. L. A. Wainstein and V. D. Zubakov, *Extraction of Signals from Noise,* Englewood Cliffs, NJ: Prentice-Hall, 1962.

2. C. H. Cook and M. Bernfeld, *Radar Signals, An Introduction to Theory and Application,* Boston: Artech House, 1993.
3. A. D. Whalen, *Detection of Signals in Noise,* New York: Academic Press, 1971.
4. D. O. North, An analysis of the factors which determine signal/noise discrimination in pulsed carrier systems. *Proc. IEEE,* **51**: 1016, 1963.
5. J. C. Mather et al., A preliminary measurement of the cosmic microwave background spectrum by the cosmic background explorer (COBE) satellite, *Astrophys. J. Lett.,* **37**: 354–356, 1990.
6. D. G. Blair et al., High sensitivity gravitational wave antenna with parametric transducer readout, *Phys. Rev. Lett.,* **74**: 1908–1911, 1995.
7. P. R. Saulson, *Fundamentals of Interferometric Gravitational Wave Detectors,* Singapore, World Scientific, 1994.
8. E. N. Ivanov, M. E. Tobar, and R. A. Woode, Microwave interferometry: Application to precision measurements and noise reduction techniques, *IEEE Trans. Microw. Theory Tech.,* 1998.
9. E. N. Ivanov, M. E. Tobar, and R. A. Woode, A study of noise phenomena in microwave components using an advanced noise measurement system, *IEEE Trans. Ultrason. Ferroelectr. Freq. Control,* **44**: 161–163, 1997.
10. R. H. Dicke, The measurement of thermal radiation at microwave frequencies, *Rev. Sci. Instrum.,* **17**: 268–275, 1946.
11. J. Randa et al., International Comparison of Thermal Noise-Temperature Measurements at 2, 4, and 12 GHz. Communicated at CPEM, Gaithersburg, MD, 1998.
12. National Physics Laboratory, Teddington, UK. http://www.npl.co.uk/npl/cetm/rfm/rfcontacts.html
13. National Institute for Science and Technology, Boulder, Colorado, USA. http://www.boulder.nist.gov/div813/81306/noise/noise.htm
14. Laboratoire Central des Industries Electriques, Fontenay-aux Roses, France. http://www.ccip.fr/club/92/lcie-gb_ps.html
15. Physikalisch-Technische Bandesanstalt, Braunschweig, Germany. http://www.ptb.de/english/org/2/hp.htm
16. N. Wiener, Generalized harmonic analysis, *Acta Math.,* **55**: 117, 1930.
17. A. Khintchine, Korrelations theorie der stationaren stoichastischen Prozesse, *Math. Ann.,* **109**: 604, 1934.
18. A. v. d. Ziel, *Noise in Solid State Devices and Circuits,* New York: Wiley, 1986.
19. F. Reif, *Fundamentals of Statistical and Thermal Physics,* McGraw Hill, 1981.
20. A. Einstein, Theory of Brown Motion, *Ann. Phys.,* **19**: 289, 371, 1906.
21. J. B. Johnson, Thermal agitation of electricity in conductors, *Phys. Rev.,* **32**: 97, 1928.
22. H. Nyquist, Thermal agitation of electric charge in conductors, *Phys. Rev.,* **32**: 110, 1928.
23. W. Schottky, Electric oscillations, *Ann. Phys.,* **57**: 541, 1918.
24. F. N. H. Robinson, *Noise and Fluctuations in Electronic Devices and Circuits,* Oxford: Clarendon Press, 1974.
25. J. Tucker, Quantum limited detection in tunnel junction mixers, *IEEE J. Quant. Electron.,* **15**: 1234, 1979.
26. C. K. Boggs et al., Measurement of voltage noise in chemical batteries, *Proc. IEEE Int. Freq. Control Symp.,* 367–374, 1995..
27. K. Amberiadis, G-R and 1/*f* noise in semiconductor devices, Ph.D. Thesis, University of Minnesota, 1982.
28. P. H. Handel, 1/*f*—an "inferred" phenomenon, *Phys. Rev. Lett.,* **34**: 1492, 1975.
29. P. H. Handel, Quantum approach to 1/*f* noise, *Phys. Rev.,* **22**: 745, 1980.
30. K. M. v. Vliet, P. H. Handel, and A. v. d. Ziel, Superstatistical emission noise, *Physica A,* **108**: 511, 1981.
31. F. N. Hooge, 1/*f* noise is no surface effect, *Phys. Lett. A.,* **29**: 139, 1969.
32. Hooge, 1/*f* noise, *Physica B,* **83**: 19, 1976.
33. R. P. Jindal and A. v. d. Ziel, Phonon fluctuation model for flicker noise in elemental semiconductors, *J. Appl. Phys.,* **52**: 2884, 1981.
34. A. L. McWhorter, 1/*f* Noise and Related Surface Effects in Germanium, Lincoln Lab., Boston 80, May 1955.
35. G. Giralt, J. C. Martin, and F. X. Matea-Perez, Sur un phénomène de bruit dans les transistors, caractérisé pas des crenaux de courant d'amplitude constante, *Compt. Rend. Acad. Sci. Paris,* **261**: 5350, 1965.
36. S. Machlup, Noise in semiconductors: spectrum of two-parameter random signal, *J. Appl. Phys.,* **25**: 341, 1954.
37. M. Mihaila and K. Amberiadis, Noise phenomena associated with dislocations in bipolar transistors, *Solid State Electron.,* **26**: 109, 1983.
38. D. F. Wait, Thermal noise from a passive linear multiport, *IEEE Trans. Microw. Theory Tech.,* **16**: 687–691, 1968.
39. H. T. Friiss, Noise figures of ratio receivers, *Proc. IRE,* **32**: 419, 1944.
40. D. F. Wait, Comments Concerning on Wafer Noise Parameter Measurements, presented at 36th ARFTG Conf. Digest, Monterey, CA, 1990.
41. T. Nemoto and D. F. Wait, Microwave circuit analysis using the equivalent generator concept, *IEEE Trans. Microw. Theory Tech.,* **16**: 866–873, 1968.
42. G. F. Engen, A new method of characterizing amplifier noise performance, *IEEE Trans. Instrum. Meas.,* **19**: 344–349, 1970.
43. D. F. Wait and G. F. Engen, Application of radiometry to the accurate measurement of amplifier noise, *IEEE Trans. Instrum. Meas.,* **40**: 433–437, 1991.
44. H. Rothe and W. Dahlke, Theory of noisy fourpoles, *Proc. IRE,* **44**: 811–818, 1956.
45. H. A. Haus and R. Q. Lane, Representation of noise in linear twoports, *Proc. IRE,* 69–74, 1959.
46. R. Q. Lane, The determination of device noise parameters, *Proc. IEEE,* **57**: 1461–1462, 1969.
47. M. Pospieszalski et al., Comments on 'Design of microwave GaAs MESFET's for broadband, low noise amplifier,' *IEEE Trans. Microw. Theory Tech.,* **34**: 194, 1986.
48. A. Cappy, Noise modelling and measurement techniques, *IEEE Trans. Microw. Theory Tech.,* **36**: 1–10, 1988.
49. E. Strid, Measurements of losses in noise matching networks, *IEEE Trans. Microw. Theory Tech.,* **29**: 247–252, 1981.
50. A. C. Davidson, B. W. Leake, and E. Strid, Accuracy improvements in microwave noise parameter measurements, *IEEE Trans. Microw. Theory Tech.,* **37**: 1973–1978, 1989.
51. D. F. Wait and J. Randa, Amplifier noise measurements at NIST, *IEEE Trans. Instrum. Meas.,* **46**: 482–485, 1997.
52. V. Adamian and A. Uhlir, A novel procedure for receiver noise characterization, *IEEE Trans. Instrum. Meas.,* **22**: 181–182, 1973.
53. W. C. Daywitt, Design and error analysis for the WR10 thermal noise standard, *Natl. Bur. Stand. (US) Technol. note 1071,* 1983.
54. W. C. Daywitt, The noise temperature of an arbitrarily shaped microwave cavity with application to a set of millimeter wave primary standards, *Metrologia,* **30**: 471–478, 1994.
55. J. Randa, Noise-temperature measurement system for the WR-28 band, *Natl. Inst. Stand. Technol. Tech. note 1395,* 1997.
56. J. S. Wells, W. C. Daywitt, and C. K. S. Miller, Measurement of effective temperatures of microwave noise sources, *IEEE Trans. Instrum. Meas.,* **13**: 17–28, 1964.

57. F.-I. Buchholz and W. Kessel, A primary broad-banded coaxial thermal noise standard for the range 100 MHz to 10 GHz, *IEEE Trans. Instrum. Meas.,* **36**: 474–479, 1987.

58. M. W. Sinclair and A. M. Wallace, A new national electrical noise standard in the X-band, *IEEE Proc. A.,* **133**: 272–274, 1986.

59. W. C. Daywitt, A reference noise standard for millimeter waves, *IEEE Trans. Microw. Theory Tech.,* **21**: 845–847, 1973.

60. M. S. Gupta et al., Microwave noise characterization of GaAs MESFET's: Evaluation by on-wafer low-frequency output of noise current measurement, *IEEE Trans. Microw. Theory Tech.,* **35**: 1208–1218, 1987.

61. L. Dunleavy, A Ka-band on-wafer s-parameter and noise figure measurement system, *Proc. 34th ATFTG Conf. Digest,* Ft. Lauderdale, FL, 1989.

62. G. Dambrine et al., A new method for on-wafer noise measurement, *IEEE Trans. Microw. Theory Tech.,* **41**: 375–381, 1993.

63. A. Boudiaf, C. Dubon-Chevallier, and D. Pasquet, Verification of on-wafer noise parameter accuracy, *IEEE Trans. Instrum. Meas.,* **44**: 332–335,1995.

64. J. Randa, R. L. Billinger, and J. L. Rice, On-wafer measurements of noise temperature, submitted to *IEEE Trans. Instrum. Meas.,* 1998.

65. J. Randa, Noise temperature measurements on-wafer, *Natl. Inst. Stand. Technol. Tech. note 1390,* 1997.

66. F. G. Ascarrunz, E. S. Ferre, and F. L. Walls, Investigations of AM and PM noise in X-band devices, *Proc. IEEE Frequency Control Symp.,* 1993.

67. T. E. Parker, Characteristics and sources of phase noise in stable oscillators, *Proc. 41st IEEE Frequency Control Symp.,* 1987.

68. M. C. Delgado Aramburo et al., Comparison of 1/*f* noise in commercial amplifiers, *Proc. IEEE Freq. Control Symp.,* 470–477,1997

MICHAEL E. TOBAR
The University of Western Australia

ELECTRIC NOISE MEASUREMENT. See NOISE, HIGH-FREQUENCY.

ELECTRIC POWER. See ELECTRICITY SUPPLY INDUSTRY.

ELECTRIC POWER FLOW. See POWER FLOW.

ELECTRIC POWER SYSTEMS. See POWER TRANSMISSION NETWORKS.